J., McCarthy, B. J., Mahley, R. W., Levy-Wilson, B., & Scott, J. (1986) *Nature 323*, 734–738.
Kostner, G. M., Avogaro, P., Cazzolato, G., Marth, E., Bittolo-Bon, G., & Quinci, G. B. (1981) *Atherosclerosis 38*, 51–61.
Laemmli, U. K. (1970) *Nature 227*, 680–682.
Liu, C. Y., & Wallen, P. (1984) *Circulation 70 (Suppl. II)*, 365.
Loscalzo, J., Freedman, J., Rudd, M. A., & Vaughan, D. E. (1987) *Arteriosclerosis 7*, 450–455.
Loscalzo, J., Weinfeld, M., Fless, G. M., & Scanu, A. M. (1990) *Arteriosclerosis 10*, 240–245.
Lowry, O. H., Rosebrough, N. J., Farr, A. L., & Randall, L. (1951) *J. Biol. Chem. 193*, 265–275.
McFarlane, A. S. (1958) *Nature 182*, 58.
McLean, J. W., Tomlinson, J. E., Kuang, W. J., Eaton, D. L., Chen, E. Y., Fless, G. M., Scanu, A. M., & Lawn, R. M. (1988) *Nature 330*, 132–137.
Miles, L. A., Fless, G. M., Levin, E. G., Scanu, A. M., & Plow, E. F. (1989) *Nature 339*, 301–302.
Murai, A., Miyahara, T., & Fujimoto, N. (1986) *Atherosclerosis 59*, 199–204.
Petersen, T. E., Martzen, M. R., Ichinose, A., & Davie, E. W. (1990) *J. Biol. Chem. 265*, 6104–6111.
Ranby, M. (1982) *Biochim. Biophys. Acta 704*, 461–469.
Rath, M., Neindorf, A., Tjark, R., Dietel, M., Krebber, H., & Beisiegel, U. (1989) *Atherosclerosis 9*, 579–592.
Rhoads, G. G., Dahlen, G., Berg, K., Morton, N. E., & Dannenberg, A. L. (1986) *J. Am. Med. Assoc. 256*, 2540–2544.
Shepard, J., Bradford, D. K., & Morgan, H. G. (1976) *Clin. Chim. Acta 66*, 97–109.
Vaughan, D. E., Mendelsohn, M. E., Declerck, P. J., van Houtte, E., Collen, D. E., & Loscalzo, J. (1989) *J. Biol. Chem. 264*, 15869–15874.
Young, S. G., Witztum, J. L., Casal, D. C., Curtiss, L. K., & Bernstein, S. (1986) *Arteriosclerosis 6*, 178–188.
Zawadzki, Z., Terce, F., Seman, L. J., Thealis, R. T., Breckenridge, W. C., Milne, R. W., & Marcel, Y. L. (1988) *Biochemistry 27*, 8474–8481.

Comparison of Operator-Specific and Nonspecific DNA Binding of the λ *cI* Repressor: [KCl] and pH Effects†

Donald F. Senear* and Robert Batey‡
Department of Molecular Biology and Biochemistry, University of California, Irvine, California 92717
Received January 7, 1991; Revised Manuscript Received April 3, 1991

ABSTRACT: The effects of proton and KCl activity on the nonspecific λ *cI* repressor–DNA interactions and on the site-specific repressor–O_R interactions were compared, in order to assess their roles in site specificity. The repressor–O_R interactions were studied by using DNase I footprint tiration. The Gibbs free energy changes for binding and for cooperativity were determined between 25 and 300 mM KCl, from individual-site isotherms for the binding of repressor to O_R and to reduced-valency mutants. The proton-linked effects on repressor–O_R interactions have been published [Senear, D. F., & Ackers, G. K. (1990) *Biochemistry 29*, 6568–6577; Senear, D. F., & Bolen, D. W. (1991) *Methods Enzymol.* (in press)]. Nonspecific binding was studied by using a nitrocellulose filter binding assay, which proved advantageous in this case, due to the relatively weak nonspecific binding, and precipitation of repressor–DNA complexes. Filter binding provided measurements at low binding density where precipitation did not occur. The data provide estimates of the Gibbs free energy changes for nonspecific, intrinsic binding, but not for cooperativity. The KCl concentration dependencies of the intrinsic binding constants indicate that ion release plays similar roles in distinguishing between the operators and in discriminating operator from nonoperator DNA. Binding to DNA is accompanied by net proton absorption. Near neutral pH, proton linkages to operator and nonoperator binding are the same. Differences at acid and at basic pH implicate the same ionizable repressor groups in distinguishing between the operators and in discriminating operator from nonoperator DNA. The results indicate similar overall modes of operator and nonoperator binding of repressor, but implicate indirect effects of DNA sequence as important contributors to sequence recognition.

The key steps in the regulation of developmental and metabolic pathways often occur at the level of initiation of transcription. In both prokaryotes and eukaryotes, this regulation involves DNA sequence dependent interactions between regulatory proteins and DNA. Due to enormous effort expended in recent years, a few general principals of sequence-specific recognition of DNA by regulatory proteins have emerged. However, a complete picture remains elusive. While it was felt, at one time, that specificity must arise strictly from contacts to functional groups in the major groove of the DNA, it is now recognized that interactions with the backbone are also important to specificity, due to sequence-dependent variations in DNA conformation and susceptibiity to protein-induced deformation of DNA [see Steitz (1990) and

†This work was supported by National Institutes of Health Grant GM41465. Undergraduate research funds from the Committee for Instructional Development at UCI were provided to R.B.
*Author to whom correspondence should be addressed.
‡Present address: Department of Biology, Massachussetts Institute of Technology, Cambridge, MA 02139.

0006-2960/91/0430-6677$02.50/0

Harrison and Aggarwal (1990) for recent reviews]. The complexity inherent in this situation raises the possibility of functionally important interactions which may not be simply interpretable in terms of local structural features.

An important example of regulation of development at the level of transcription initiation, one in which site-specific binding plays a central role, is provided by the right operator (O_R)[1] of the bacteriophage λ. The interactions of the phage-encoded *c*I and *cro* repressors with three operator sites at O_R constitute the primary control of the switch from lysogenic to lytic phage cycles [see Johnson et al. (1981) for a review]. Two features which are crucial to this regulation are (i) the differential affinities of the λ *c*I and *cro* repressors for their operator sites (Meyer, et al., 1980) and (ii) the cooperative interactions between *c*I repressors bound at different operator sites (Johnson et al., 1979; Shea & Ackers, 1985). Site specificity can be considered to operate at two levels in this system. First is the specificity for operator sequences, as opposed to random-sequence DNA; second is the differential affinity for different operators. Cooperativity certainly plays a role in the latter, i.e., in modulating the effective affinity of O_R2 versus O_R3 (see below). Its role in the former has not been ascertained.

The present study was stimulated by the demonstration of operator site-specific pH effects on the *c*I repressor–O_R interactions (Senear & Ackers, 1990) which provide part of the energy for the differential affinity of the repressor for the three operator sites of O_R. The conclusion that this represents an effect of DNA conformation is supported by the lack of appropriate ionizable groups that contact the DNA (Jordan & Pabo, 1988). Here, we report on the effects of monovalent salt concentration on the repressor–operator interactions. The entropic contribution from removal of cations and water from the DNA upon protein binding generally provides a large fraction of the overall binding energy (Record et al., 1985) and so might be expected to be sensitive to site-specific differences in the interactions of the repressor with the DNA backbone. In addition, we have also studied the effects of pH and of monovalent salt concentration on the *nonspecific* binding of the repressor to nonoperator DNA, to determine whether similar interactions are involved at both levels of specificity.

The cooperative, site-specific repressor–O_R interactions were studied by using quantitative footprint titration. At each concentration of monovalent salt (25–300 mM KCl), individual-site titration data for O_R wild-type and for three reduced-valency mutants were analyzed to resolve the Gibbs free energy changes both for binding to each of the operator sites and for cooperativity (Senear et al., 1986; Senear & Ackers, 1990). The nitrocellulose filter binding assay was used to study the nonspecific interactions of repressor with non-operator-bearing DNA fragments derived from pBR322. While these data did not allow for rigorous examination of potential cooperativity in nonspecific binding, they did provide precise estimates of the free energy change for intrinsic DNA binding.

The results of these studies indicate significant variation in the stoichiometry of ion participation in the binding of repressor to the three operator sites. The stoichiometry of ion participation in nonspecific binding lies in the middle of the range obtained for the operators. The overall pattern of linkage between proton binding and nonspecific protein–DNA binding is similar to that for operator binding. However, the same groups that are involved in distinguishing between the three operator sites appear also to be involved in discriminating operator DNA. These observations implicate similar "indirect readout" type interactions as playing a significant role in site specificity at both levels. A transition near 0.1 M KCl divides conditions of high salt, where operator binding is highly cooperative, and of low salt, where it is much less so. However, within each of the two regions, cooperativity is not highly sensitive to KCl concentration. Implications regarding the mechanism of site-specific binding and regulation are discussed.

Materials and Methods

Chemical Reagents. [α-^{32}P]dNTPs (3000 Ci/mmol) were purchased from Amersham; unlabeled dNTPs were from BRL. Electrophoresis-grade acrylamide and bis(acrylamide) from Bio-Rad were deionized by using Bio-Rad AG501-x8 mixed-bed resin before use. Klenow polymerase and bovine serum albumin (BSA; acetylated, nucleic acid grade) were from BRL. Calf thymus DNA (CT-DNA) was from Sigma. Bovine pancreas deoxyribonuclease I (DNase I, code D) from Worthington was treated as described (Brenowitz et al., 1986). To maintain constant DNase I exposure, the relative catalytic activity was determined at each [KCl], essentially as described (Kunitz, 1950). The apparent activity of the enzyme varied by 2 orders of magnitude over the range of [KCl] used.[2] All other reagents were reagent or analytical grade.

Repressor Protein. λ *c*I repressor protein was purified as described (Brenowitz et al., 1986). The repressor protein preparation used is >95% pure as judged by $NaDodSO_4$–PAGE. The specific DNA binding activity is 55%, on the basis of stoichiometry experiments of the type described by Sauer (1979) and by Johnson (1980), and on $\epsilon^{280nm}_{mg/mL} = 1.18$. All repressor concentrations are expressed as total active monomer concentrations, which were calculated from the stoichiometry experiments. Repressor dimer is active in binding DNA. For experiments at 200 mM KCl, dimer concentrations were calculated on the basis of a dissociation constant, k_d, of 3.7 nM [see Senear and Ackers (1990)]. At other concentrations of KCl, k_d was calculated on the basis of a linear dependence of log k_d on log [KCl]. The slope was obtained from recent steady-state fluorescence anisotropy measurements at 50 mM KCl, from which we estimate k_d to be approximately 30 nM (J. B. A. Ross and D. F. Senear, unpublished experiments).[3]

DNA. Isolation and radiolabeling of 1107 bp DNA fragments containing either the wild-type (O_R^+) or the reduced-valency mutant λ right operators whose binding competencies are O_R1^-, O_R2^-, and $O_R1^-3^-$ were as described (Senear & Ackers, 1990). The mutant operators contain a single base pair substitution in each of the mutated sites. Non-operator-containing DNA fragments of length (measured after Klenow fill-in-labeling) 91, 225, 540, 1211, and 1749 bp were isolated from an *Ava*II and partial *Nde*I digestion of pBR322 DNA (the 1749 bp fragment results from incomplete *Nde*I

[1] Abbreviations: bis(acrylamide), *N*,*N*′-methylenebis(acrylamide); Bistris, [bis(2-hydroxyethyl)amino]tris(hydroxymethyl)methane; BRL, Bethesda Research Labs; BSA, bovine serum albumin; bp, base pair(s), CT-DNA, calf thymus DNA; DNase I, bovine pancreas deoxyribonuclease I (EC 3.1.21.1); EDTA, (ethylenedinitrilo)tetraacetic acid; $NaDodSO_4$, sodium dodecyl sulfate; O_R, λ right operator; Tris, tris(hydroxymethyl)aminomethane.

[2] Activity decreased with increasing [KCl]. The specificity of the enzyme, as indicated by the banding pattern observed in footprint autoradiograms, was unaffected by [KCl]. On the basis of these observations, we conclude that the change in apparent affinity primarily reflects the expected [KCl] effect on the binding of DNase I to DNA, rather than an effect on specific activity.

[3] See Casali et al. (1991) for methods.

digestion). The pBR322 sequence was searched to ensure the lack of any significant sequence similarity to the λ operator sequences. DNA fragments were agarose or acrylamide gel purified from CsCl gradient banded plasmid preparations and were essentially free of protein, as determined from the A_{260}/A_{280} ratio (Maniatis et al., 1982). The specific radioactivity of freshly labeled operator DNA [(5–9) × 10^6 Ci/mol] was used to estimate the operator concentration in binding experiments, where necessary.

Highly polymerized CT-DNA used as carrier DNA in nonspecific binding experiments was solubilized by brief sonication. The resulting distribution of fragments (ca. 500–5000 bp) was fractionated by agarose gel electrophoresis. Separate fractions representing 250 bp (below 2000 bp) or 500 bp ranges in fragment size (e.g., 1750–2000 and 2000–2500 bp) were isolated. The size ranges were confirmed by electrophoresis of the separate fractions.

Individual-Site Binding Experiments. Quantitative DNase I footprint titrations were conducted essentially as described (Brenowitz & Senear, 1989; Senear & Ackers, 1990). Experiments were conducted in a buffer (assay buffer) consisting of 10 mM Bistris (pH 7.00 ± 0.01), 25–400 mM KCl, 2.5 mM $MgCl_2$, 1.0 mM $CaCl_2$, 0.1 mM Na_4EDTA, 100 μg/mL BSA, and 2 μg/mL (non-size-fractionated) CT-DNA. The pH of each buffer was adjusted with HCl at the temperature of the experiments (20 ± 0.1 °C). Reaction mixtures (300 μL) were equilibrated in a water bath for between 40 min and 2 h prior to binding assays. Binding measurements are independent of the incubation time over this range.

Conditions for DNase I exposure were 0.3–30 ng of DNase I (depending on the apparent activity of the enzyme at a given [KCl]) added in a 5.0-μL volume, for 8.0 min. DNase I reactions were quenched before addition of stop solution (Brenowitz & Senear, 1989), by addition of one-sixth volume of 50 mM Na_4EDTA. Two-dimensional optical scanning of footprint titration autoradiograms at a resolution of 210 μm × 210 μm was accomplished by using an Eikonix 78/99 2048 element photodiode array camera controlled by a MicroVAX 3200 computer. The optical resolution is 0–1.60 ODU in 256 steps. Graphically interfaced programs were developed in this lab for the camera control and analysis of the digitized autoradiogram images.

Nonspecific Binding Experiments. The nonspecific binding of the repressor to the pBR322 DNA fragments was monitored by using the nitrocellulose filter binding assay, in the assay buffer described above, except that Tris and potassium acetate were substituted for Bistris above pH 7 and below pH 6, respectively. Aliquots of 45 μL (from 50-μL reaction mixtures) were applied to the filters. The filtering, washing, and scintillation counting were essentially as described (Senear et al., 1986).

Filters (0.45 μm, 25-mm circles obtained from Schleicher & Schuell) were treated by soaking for 10 min in 0.4 N NaOH, followed by soaking in wash buffer (assay buffer, less BSA and CT-DNA) for 1–2 h before use. Pretreatment decreased background retention of radiolabeled DNA in the absence of repressor. Still, a minimum concentration of carrier CT-DNA was required to prevent excessive background retention. At the concentrations used (usually 0.1 μg/mL), backgrounds were typically 5% of the total cpm. Since even this CT-DNA concentration represents a substantial excess over the concentration of pBR322 fragment DNA (ca. 20–200-fold depending on the pBR322 fragment size), the appropriate size-fractionated CT-DNA was used (e.g., 1500–2000 bp for the experiments using the 1759 bp pBR322 fragment). In this way, a reasonably homogeneous mix of fragment sizes was present in any experiment.

Table I: Microscopic Configurations and Associated Free Energy States for the λ cI Repressor–O_R System[a]

species	operator configurations: site 1	site 2	site 3	free energy contributions	total free energy
1	O	O	O	reference state	ΔG_{s1}
2	R_2	O	O	ΔG_1	ΔG_{s2}
3	O	R_2	O	ΔG_2	ΔG_{s3}
4	O	O	R_2	ΔG_3	ΔG_{s4}
5	R_2 ↔	R_2	O	$\Delta G_1 + \Delta G_2 + \Delta G_{12}$	ΔG_{s5}
6	O	R_2 ↔	R_2	$\Delta G_2 + \Delta G_3 + \Delta G_{23}$	ΔG_{s6}
7	R_2	O	R_2	$\Delta G_1 + \Delta G_3$	ΔG_{s7}
8	R_2 ↔	R_2 ↔	R_2	$\Delta G_1 + \Delta G_2 + \Delta G_3 + \Delta G_{123}$	ΔG_{s8}

[a] Operator sites are denoted by O if vacant or by R_2 if occupied by cI repressor dimers. Cooperative interactions are denoted by (↔). The total Gibbs free energy of each configuration (ΔG_s) relative to the unliganded reference state is shown as the sum of contributions from six energy changes. ΔG_i values (i = 1, 2, or 3) are the intrinsic free energy changes for binding to the operator sites; $\Delta G_{ij(k)}$ values are the free energy changes due to cooperative interaction between liganded sites, defined as the difference in free energy change to fill the sites simultaneously (ΔG_T) and the free energy change to fill them individually ($\sum_i \Delta G_i$). The free energy changes are related to the corresponding microscopic equilibrium constants, k_i, by the standard thermodynamic relationship $\Delta G_i = -RT \ln k_i$.

Numerical Analysis. All experimental data were analyzed according to the appropriate quantitative expressions by using nonlinear least-squares methods of parameter estimation. The analysis program (Johnson & Frasier, 1985) uses a variation of the Gauss–Newton procedure (Hildebrand, 1956) to determine the best-fit, model-dependent parameter values that correspond to a minimum in the variance. The N-dimensional parameter space is searched for the variance ratio predicted by an F statistic (Box, 1960) to determine the worst case joint-confidence limits for the fitted parameters. The confidence limits correspond to approximately one standard deviation.

A statistical mechanical model for the interaction of the cI repressor with O_R has been thoroughly evaluated (Senear & Ackers, 1990). The salient features of this model are represented by the configurations listed in Table I. The individual-site binding equation for each operator site is constructed by considering the relative probability for each configuration with repressor bound to that site (Ackers et al., 1982, 1983). For the wild-type operator, the fractional occupancies of the sites are given by

$$\bar{Y}_{O_R1} = f_2 + f_5 + f_7 + f_8 \quad (1a)$$

$$\bar{Y}_{O_R2} = f_3 + f_5 + f_6 + f_8 \quad (1b)$$

$$\bar{Y}_{O_R3} = f_4 + f_6 + f_7 + f_8 \quad (1c)$$

where f_s is the fractional probability of one operator configuration, given by

$$f_s = \frac{e^{-\Delta G_s/RT} R_2^j}{\sum_{sj} e^{-\Delta G_s/RT} R_2^j} \quad (2)$$

ΔG_s is the sum of free energy contributions for configuration "s" (Table I), R is the gas constant, T is the absolute temperature, R_2 is the concentration of free repressor dimer, and j is the number of ligands bound in to configuration "s". At most conditions, the concentration of operator DNA used (less than 20 pM) was sufficiently low to ignore the difference between free and total repressor concentrations. At the conditions of highest affinity where the difference could not be safely ignored, the full conservation equation for repressor was utilized, as described (Senear & Ackers, 1990).

Since even saturating protein ligand does not confer absolute protection, the quantity that is obtained in the footprint experiment is not $\bar{Y}_{O_Ri}$, but rather the fractional protection of the site, denoted by P_{O_Ri}. The P_{O_Ri} values are linearly related to, but not equal to, $\bar{Y}_{O_Ri}$ (Brenowitz et al., 1986). Thus, the final form of the equations used in the nonlinear least-squares fitting is

$$P_{O_Ri,obs} = P_{O_Ri,o} + (P_{O_Ri,f} - P_{O_Ri,o})\bar{Y}_{O_Ri} \quad (3)$$

where $P_{O_Ri,o}$ and $P_{O_Ri,f}$ are fitted lower and upper end points to the observed transition curves, respectively.

Simultaneous analysis of binding data for O_R and to reduced-valency mutants whose binding competencies are O_R1^-, O_R2^-, and $O_R1^-3^-$ was used to resolve unique values of the six interaction energies (Table I) at each experimental condition (Ackers et al., 1982; Senear et al., 1986). Binding expressions for the mutant operators are constructed in the manner described above, except that only those configurations applicable to the mutant are considered. This formulation assumes that the interactions at the remaining site(s) are quantitatively unaffected by the mutation(s). The methods used in the simultaneous analyses, including the calculation of normalized weighting factors to account for variable experimental noise in the different isotherms, have been described in detail (Senear & Bolen, 1991).

Filter binding separates liganded from unliganded DNA as described by Clore et al. (1982):

$$\theta = [DNA_{bound}]/[DNA_{total}] = Z - 1/Z \quad (4)$$

Z is the binding polynomial (Wyman, 1964) given by $Z = \sum_{j=0}^{n} K_j R_Z^j$, where K_j is the macroscopic binding constant for the binding of j ligands. The equation for K_j that contains the combinatorial factors that account for binding site overlap in the nonspecific binding of a protein to a finite-length DNA (Woodbury & von Hippel, 1983) is

$$K_j = k_i^j \sum_{l=1}^{j} \frac{(N - j\bar{n} + 1)!(j-1)!\omega^{l-1}}{(N - j\bar{n} - j + 1)!(j - l + 1)(l - j)!(j-1)!} \quad (5)$$

where k_i is the intrinsic, microscopic binding constant for each DNA site, N is the size (in base pairs) of the DNA, $\bar{n}$ is the site size (base pairs occluded by binding of one ligand), and ω is a cooperativity parameter, which accounts for the free energy of cooperative interaction when ligands bind at contiguous sites. In analyzing our experimental data, it was necessary to account for the fact that less than 100% of the DNA is retained by the filters at saturation with repressor (cf. Figure 6, below). Thus, the final form of the equation used was

$$D_{obs} = D_{tot}(\sum_{j=1}^{n} K_j R_Z^j r_j)/Z + D_o \quad (6)$$

where D_{tot} and D_o are the total DNA applied to the filter and the background retention, respectively, n is the maximum number of ligands that can bind, given by $N/\bar{n}$, and r_j is the retention for a complex with j ligands bound. Different formulations for r_j were considered, as described below.

Results

[KCl] Dependence of Site-Specific, Repressor–O_R Interactions. The cooperative, site-specific interactions of the *c*I repressor and O_R were studied by using the DNase I footprint method (Brenowitz et al., 1986). Figure 1 presents data for the binding of repressor to O_R at 50 mM KCl. The solid curves drawn through the points represent the results of the simultaneous analysis of these data, and also of data from titration experiments conducted on reduced-valency mutant operators

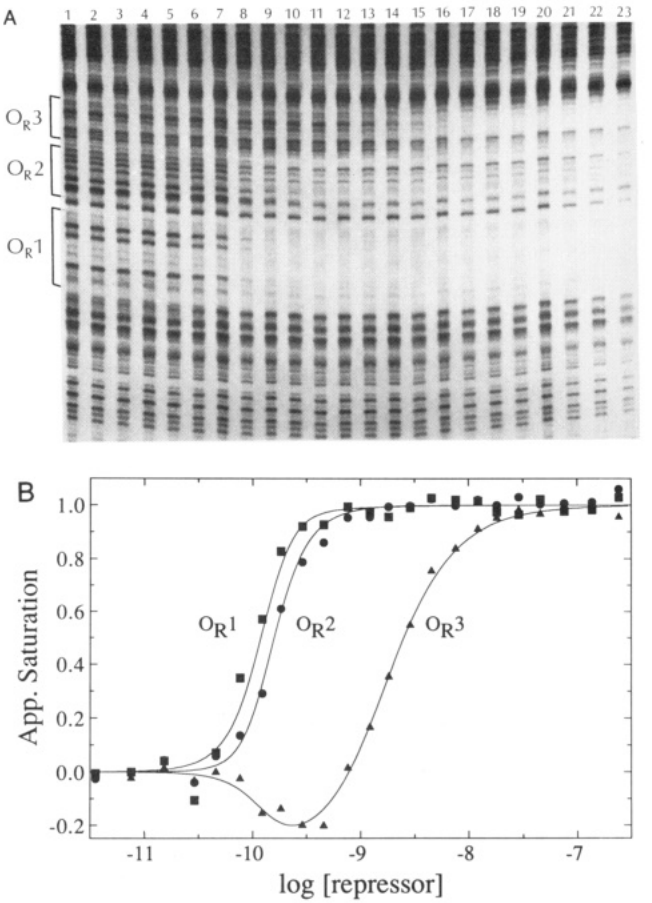

FIGURE 1: Footprint titration of *c*I repressor binding to O_R at 20 °C, 50 mM KCl, pH 7.0, standard assay buffer (Materials and Methods). (A) Autoradiogram of the DNA after exposure to DNase I. Regions corresponding to the operator sites O_R1, O_R2, and O_R3 are marked. Lane 1 is the reference (no repressor) for calculation of fractional protection. Lanes 2–23 show approximately even log increments in repressor concentration from 7.6×10^{-12} to 2.4×10^{-7} M. (B) Extent of saturation for sites O_R1 (squares), O_R2 (circles), and O_R3 (triangles) from the data in (A). Hypersensitivity in O_R3 mimics the apparent *negative* fractional saturation (see text); the abscissa is labeled App. Saturation in acknowledgement. The solid lines through the points represent the simultaneous analysis of binding data for the wild-type and reduced-valency mutant operators as in Figure 2. Estimated Gibbs free energy changes for the interactions are in Table II.

(see below) according to the model given in Table I. The precision of the data and the correspondence between the model-dependent curves and the data are representative of all conditions studied.

A pronounced dip in the O_R3 data at intermediate repressor concentrations results from hypersensitivity to DNase I in O_R3, relative to the absence of repressor. This hypersensitivity is strongly [KCl] dependent, diminishing in intensity to near zero by 200 mM KCl (see Figure 3, below). It is also observed in titrations of O_R2^- DNA (see Figure 2, below) but is not observed in other sites or other operators. The increased rate of DNase I catalyzed cleavage in O_R3 appears to be a direct consequence of repressor binding to O_R1. A similar conclusion was reached independently by Strahs and Brenowitz (1990). The negative values of apparent fractional saturation are a consequence of the normalization of the fractional protection data to the lane with zero repressor (Brenowitz et al., 1986). In the normalization procedure, protection, seen as a decrease in OD, is due to repressor ligation. Therefore, hypersensitivity necessarily yields apparent negative fractional saturation.

To account quantitatively for this effect, a third end point ($P_{O_R3,h}$), reflecting the apparent decrease in the fractional

Table II: [KCl] Effects on Microscopic Gibbs Free Energy Changes of *c*I Repressor–O_R Interactions[a]

[KCl] (mM)	ΔG_1	ΔG_2	ΔG_3	ΔG_{12}	ΔG_{23}	ΔG_{123}	σ[b]
25	−17.4 ± 0.2	−16.2 ± 0.2	−13.6 ± 0.4	−0.9 ± 0.3	−2.6 ± 0.5	−2.1 ± 0.6	0.057
50	−16.2 ± 0.2[c]	−14.9 ± 0.2	−12.1 ± 0.3	−1.6 ± 0.3	−2.8 ± 0.5	−2.9 ± 0.6	0.063
75	−14.8 ± 0.2	−13.1 ± 0.1	−12.0 ± 0.2	−2.4 ± 0.3	−3.2 ± 0.3	−2.9 ± 0.4	0.054
100	−14.2 ± 0.4	−13.5 ± 0.2	−11.9 ± 0.4	−1.7 ± 0.6	−1.8 ± 0.5	−1.6 ± 0.7	0.070
150	−13.3 ± 0.2	−12.3 ± 0.2	−11.0 ± 0.7	−3.6 ± 0.4	−3.2 ± 0.7	−4.8 ± 0.9	0.065
200	−12.8 ± 0.3	−11.0 ± 0.3	−9.9 ± 0.5	−3.0 ± 0.5	−3.6 ± 0.8	−3.5 ± 1.0	0.073
300	−10.8 ± 0.3	−9.6 ± 0.4	−9.4 ± 0.4	−4.9 ± 0.5	−3.4 ± 0.7	−5.2 ± 0.9	0.083
400	nd[d]	−8.5 ± 0.5	nd	nd	nd	nd	0.050

[a] Standard Gibbs free energy changes (in kilocalories per mole ± 65% confidence intervals; 1 cal equals 4.184 J) of the *c*I repressor–O_R interactions, obtained by simultaneous analysis of wild-type O_R and of reduced-valency mutant O_R binding data. Binding conditions were pH, 7, 20 °C, and KCl concentration as indicated. [b] Square root of the variance of the fitted curves from simultaneous analysis. [c] Nelson and Sauer (1986) obtained −15.0 kcal/mol for binding to O_R1 from the plasmid pO_R1 (Johnson, 1980) under substantially identical experimental conditions, and assuming a repressor dimer dissociation constant of 20 nM. Using the same assumption, our value is −16.0 kcal/mol. The difference is exactly as accounted for by the context-dependent effect of deleting the O_R2/O_R3 DNA from pO_R1, as described by Brenowitz et al. (1989), and the salt dependencies reported by Nelson and Sauer (1985) and in Table III. [d] Not determined. O_R2 value determined from $O_R1^-3^-$ titration data only.

protection due to hypersensitivity, and the fractional probability terms for species liganded at O_R1, but not O_R3 (i.e., species 2 and 5, Table I), were included in the binding equation for O_R3. For the wild-type operator, this gives

$$P_{O_R3,obs} = P_{O_R3,o} + (P_{O_R3,h} - P_{O_R3,o})(f_2 + f_5) + (P_{O_R3,f} - P_{O_R3,o})(f_4 + f_6 + f_7 + f_8) \quad (7)$$

The sensitivity of the fitted free energy changes to this analysis was tested by also analyzing the titration data in the normal manner, e.g., according to eq 1, 2, and 3. In these analyses, either the O_R3 data which show the hypersensitivity (e.g., the first eight points for O_R3 in Figure 1) were deleted, or the data were included and the systematic deviation between the data and the fitted curve was ignored. In no case did the estimates of any of the free energy changes from these three procedures differ from one another by greater than 0.2–0.3 kcal/mol, or about the limits of the experimental uncertainty (Table II). Of course, the variance of the fitted curves is dramatically improved by accounting for the hypersensitivity in the binding equations.

The cooperative interactions embodied in the interactions of the λ repressor with O_R (Johnson et al., 1979; Ackers et al., 1982) are evident in the steepness of the O_R1 and O_R2 isotherms (see also Figures 2 and 3 below). To resolve the

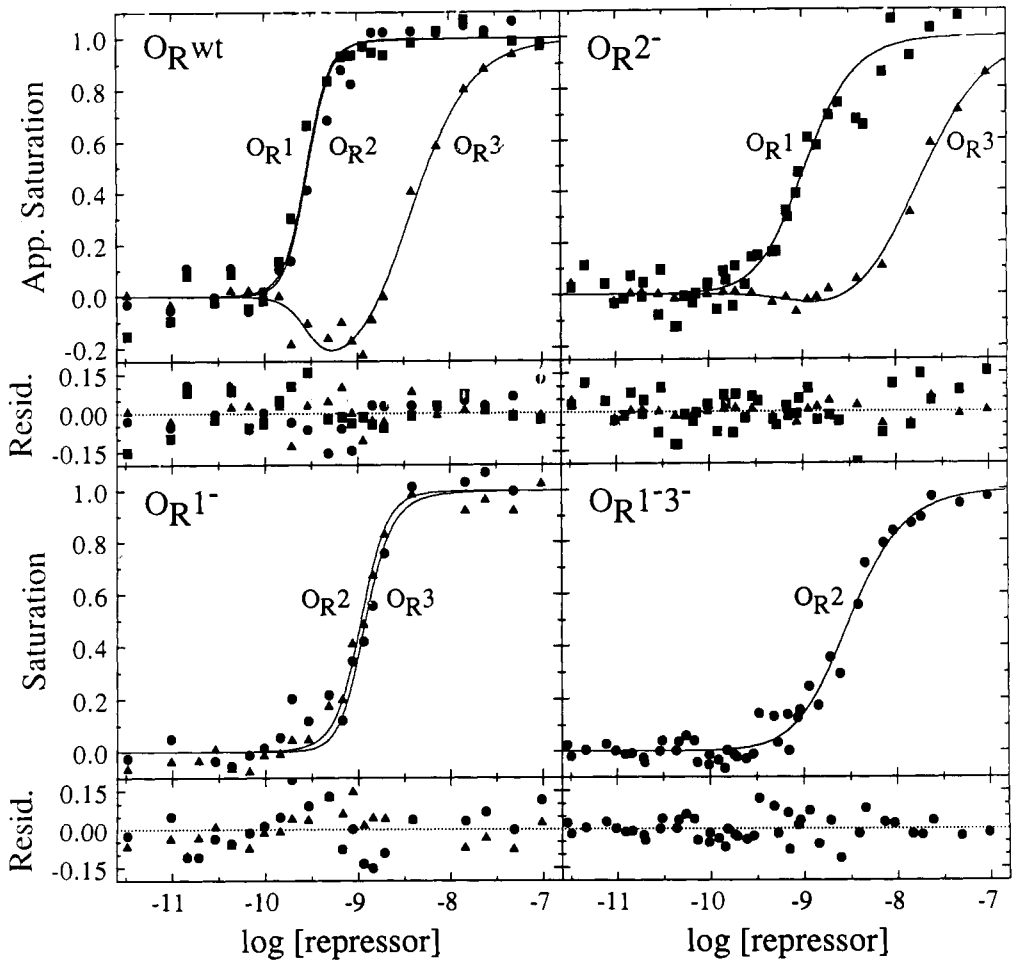

FIGURE 2: Individual-site binding of repressor to O_R and to reduced-valency mutants at 20 °C, 150 mM KCl, pH 7.0, standard assay buffer. Panels show $O_R$wt, O_R2^-, O_R1^-, and $O_R1^-3^-$, as indicated. (Squares) O_R1; (circles) O_R2; (triangles) O_R3. The curves represent the simultaneous analysis of all of the data shown using the model defined by Table I and eq 2. Estimated Gibbs free energy changes for the interactions are in Table II.

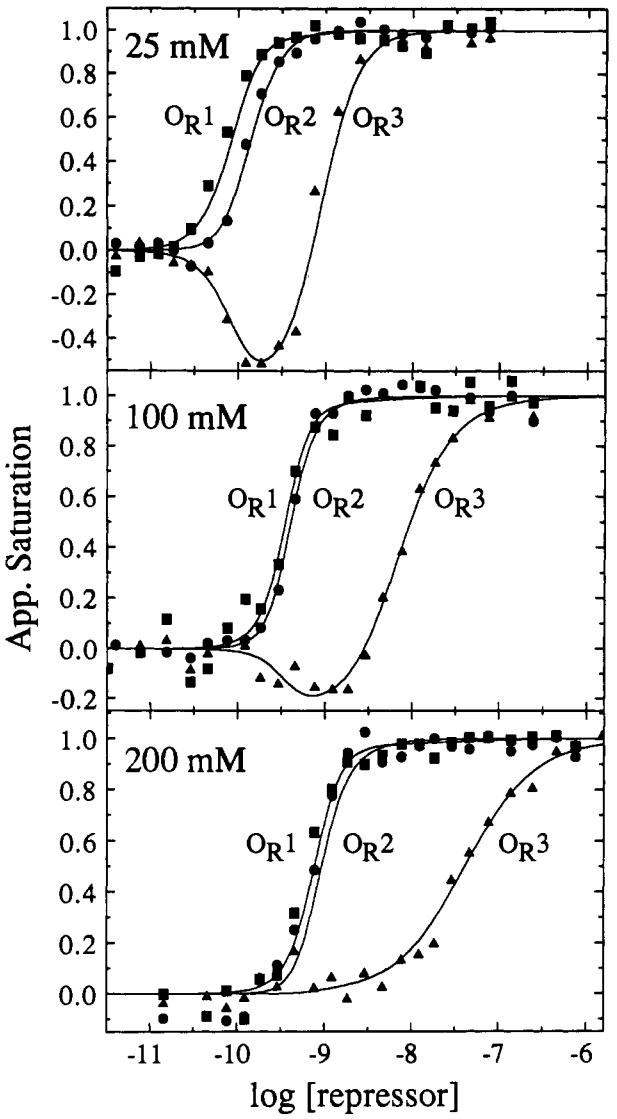

FIGURE 3: Individual-site binding data showing the effect of increasing [KCl] on cooperative interactions of *c*I repressor and O_R at 20 °C, pH 7.0, standard assay buffer. Panels show 25, 100, and 200 mM KCl as indicated. (Squares) O_R1; (circles) O_R2; (triangles) O_R3. The curves represent the simultaneous analysis of all binding data for the wild-type and reduced-valency mutant operators at each condition, as in Figure 2. Estimated Gibbs free energy changes for the interactions are in Table II.

interaction free energy changes for the model given in Table I, it is necessary to also analyze binding to reduced-valency mutants of O_R, whose binding competencies are O_R1^-, O_R2^-, and $O_R1^-3^-$ (Senear et al., 1986; Senear & Ackers, 1990).[4] The complete binding data collected for these operators at 150 mM KCl are shown in Figure 2. The data for these different operators were analyzed simultaneously as described under Materials and Methods, using the appropriate binding expressions for the model defined by Table I. The results, indicated by the solid lines in Figure 2, are listed in Table II.

Similar titration experiments were conducted over the range of KCl concentrations 25–300 mM. Representative *c*I repressor–O_R titration experiments over this range are presented in Figure 3. The solid curves represent the results of simultaneous analysis of the data shown and the reduced-valency mutant data, as discussed above. In most cases, data consisting of more than 250 points from either 5 or 6 separate titration experiments were analyzed. The free energy changes estimated from these analyses are listed in Table II. Resolution of the free energy changes for binding to the three operator sites is quite good. Uncertainties of 0.2–0.3 kcal/mol represent only a factor of 1.5 in the corresponding equilibrium constants. Estimation of the free energy changes for the cooperative interactions is less precise, since these are very sensitive to all systematic differences between different experiments for the wild-type and mutant operators. The experiments at 200 mM KCl repeat the experiments of Senear and Ackers (1990). The values obtained here are in excellent agreement with those, being well within experimental error in every case.[5]

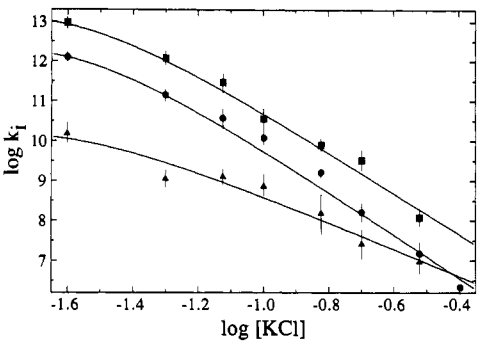

FIGURE 4: log–log plot of the [KCl] dependence of intrinsic binding of repressor to O_R at 20 °C, pH 7.0, standard assay buffer. Points plotted are microscopic equilibrium constants estimated by simultaneous analysis of individual-site binding data as shown in Figure 2. (Squares) O_R1; (circles) O_R2; (triangles) O_R3. Error bars represent the confidence limits (see Materials and Methods), corresponding to approximately one standard deviation. Solid lines are the results of simultaneous analysis of the data for the three operator sites using eq 8–10, as described in the Discussion. Parameters are listed in Table III.

A log–log of the [KCl] effect on the intrinsic binding of the repressor to the three operators is shown in Figure 4. The overall trend is a large decrease in binding affinity as the [KCl] is increased. This is in line with the expectation that counterion release from the DNA makes a substantial entropic contribution to protein binding to DNA (Record et al., 1978). Pronounced curvature in the data at low [KCl] is evident. This is a consequence of the presence of divalent metal cations (2.5 mM Mg^{2+} and 1.0 mM Ca^{2+}) in the assay buffer (Record et al., 1977). These compete with K^+, as well as with the repressor, for sites on the DNA. It was necessary to include Mg^{2+} and Ca^{2+} in the buffers for enzymatic activity of DNase I, and in order to match the conditions used in the pH studies of the repressor–O_R interactions by Senear and Ackers (1990). The slope in the limit of high [KCl] reflects the effect due to KCl alone. An important observation is that the limiting slopes are significantly different for the three sites. The KCl effect appears to be similar for O_R1 and O_R2, but much less for O_R3. The difference stands out quite clearly above the small uncertainty in the determination of the intrinsic binding parameters.

Nonspecific Repressor–DNA Binding. The nonspecific binding of the *c*I repressor to DNA was studied by using the nitrocellulose filter binding assay. Filter binding proved advantageous in this case, because, by measuring the fraction

[4] Senear and Ackers (1990) also used an $O_R1^-2^-$ operator in their analysis of pH effects on the *c*I repressor–O_R interactions. This was necessary for the testing of different models for the cooperative interactions, in particular for the question of cooperativity between O_R1 and O_R3 (ΔG_{13}). Their finding of no O_R1–O_R3 cooperative interaction confirmed the earlier report of Johnson et al. (1979) and removes the need for titrations of the $O_R1^-2^-$ operator in these studies.

[5] When analyzed by using the same dimer dissociation constant, k_d = 20 nM, as used by Senear and Ackers (1990).

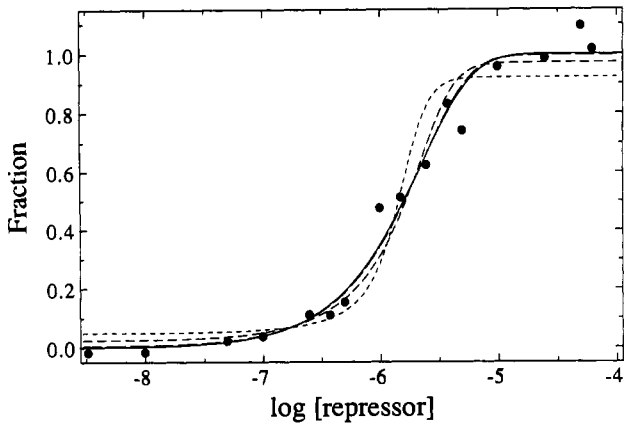

FIGURE 5: Filter binding titration of nonspecific repressor binding to the 1749 bp pBR322 *Ava*II fragment (binding conditions: 20 °C, 200 mM KCl, pH 7.0, standard assay buffer, 0.1 μg/mL CT-DNA). Data were analyzed by using eq 6 with different values of site size ($\bar{n}$) and cooperativity (ω) as described in the text. The solid line shows $\omega = 1$ and $\bar{n} = 17$, 20, and 24. The estimated Gibbs binding free energy change is -3.65 ± 0.13 kcal/mol. Square root of the variance is $\sigma = 0.064$. The dashed lines show $\bar{n} = 20$ and $\omega = 100$ ($\Delta G_i = -3.62 \pm 0.13$, $\sigma = 0.067$), $\omega = 1000$ ($\Delta G_i = -3.44 \pm 0.16$, $\sigma = 0.089$), and $\omega = 10000$ ($\Delta G_i = -2.91 \pm 0.19$, $\sigma = 0.139$) for short, medium, and long dashes, respectively.

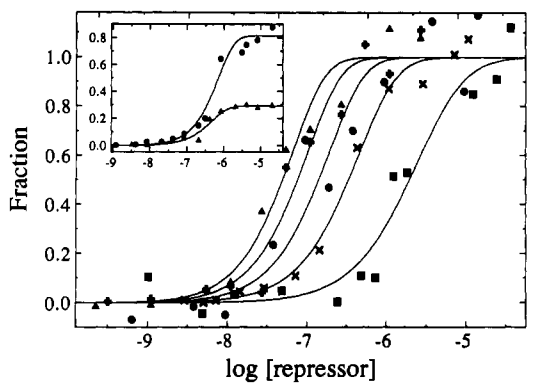

FIGURE 6: Filter binding titrations of nonspecific repressor binding to different length pBR322 fragments, showing the expected dependence for constant retention of all liganded complexes. Binding conditions: 20 °C, 100 mM KCl, pH 7.0, standard assay buffer (no CT-DNA). Solid curves are from separate analysis of each experiment using eq 6, with $\bar{n} = 20$ and $\omega = 1$, and constant retention assumed. Symbols and results are the following: (triangles) 1749 bp *Ava*II fragment ($\Delta G_i = -5.89 \pm 0.27$, $\sigma = 0.108$); (pluses) 1211 bp *Ava*II/*Nde*I fragment ($\Delta G_i = -5.81 \pm 0.27$, $\sigma = 0.114$); (circles) 540 bp *Ava*II fragment ($\Delta G_i = -5.87 \pm 0.48$, $\sigma = 0.173$); (crosses) 225 bp *Ava*II fragment ($\Delta G_i = -5.89 \pm 0.12$, $\sigma = 0.047$); (squares) 91 bp *Ava*II fragment ($\Delta G_i = -5.50 \pm 0.30$, $\sigma = 0.105$). From separate analysis of all experiments using different fragment lengths at this condition (12), $\Delta G_i = -5.83 \pm 0.19$, with constant retention assumed. The lack of CT-DNA accounts for the appreciable scatter (see Materials and Methods). (Inset) Filter binding titrations showing no effect of total retention on titration curves. Reaction conditions: 20 °C, 200 mM KCl, pH 6.5, standard assay buffer (0.1 μg/mL CT-DNA). The two titrations show 29.2% and 81.5% total retention and yield $\Delta G_i = -4.56 \pm 0.15$ kcal/mol and $\Delta G_i = -4.32 \pm 0.18$ kcal/mol, respectively.

of DNA with one or more ligands bound (θ), it assays binding at very low binding density. This avoids precipitation of the protein–DNA complexes, which we observe under all conditions of our experiments, at the higher repressor concentrations necessary for full saturation of the DNA (see Discussion). A representative filter binding titration of repressor binding to the 1749 bp pBR322 fragment is shown in Figure 5. These data were analyzed by using eq 6 as described below.

A feature of the filter binding assay for a fragment, that is much larger than the binding site size, is low sensitivity to cooperativity. This is because the number of sites at which a second ligand will bind noncooperatively (i.e., all sites not contiguous with the first ligand) is large relative to the two contiguous sites at which it binds cooperatively. To an order of magnitude approximation, the data are insensitive to $\omega \leq N$, the fragment size, which is the number of potential, noncooperative binding sites. This point is illustrated in Figure 5 which shows the results of analysis with different fixed values of ω. For $\omega \leq 1000$ ($\Delta G_\omega \geq -4.0$ kcal/mol), the fitted curves are indistinguishable and the effect on the estimated k_i (or ΔG_i) negligible. The data are sensitive to $\omega > 1000$; the quality of the fit decreases rapidly, with σ (the square root of the variance) doubling by $\omega = 10000$ ($\Delta G_\omega = -5.4$ kcal/mol). This result was also obtained at all other conditions tested. Since $\Delta G_\omega = -4.0$ kcal/mol equals or exceeds the pairwise cooperativity found in repressor–O_R interactions (Table II; Senear & Ackers, 1990) and given the expectation that cooperativity is not greater in nonspecific than in specific, operator binding, we have analyzed our data subject to the simplification $\Delta G_\omega = 0.0$.

A similar result obtains for the binding site size ($\bar{n}$, in eq 5). This is because the effects of binding site overlap and exclusion are small for the binding of the first few ligands to a large lattice. On the basis of the spacing of the operations in λ O_R and O_L, we infer a minimum nonspecific binding site size of 17 bp, the size of the operator palindrome, and a maximum of 24, equal to the palindrome plus the largest spacing between operators in O_R and O_L. This estimate of site size is also consistent with the size of the protected region in DNase I footprint experiments (cf. Figure 1). The solid line drawn through the points in Figure 5 represents the data analyzed with $\bar{n} = 17$, 20, and 24. The difference is everywhere less than the thickness of the line, justifying the further simplification, $\bar{n} = 20$.

The total retention observed in our nonspecific binding experiments varied over ca. 30–80% (depending on the filter lot) with no apparent dependence on binding conditions. Woodbury and von Hippel (1983) have proposed that the r_j (eq 6) for each complex should be given by $1 - \zeta^j$ where j is the number of ligands bound in a given complex and ζ is the probability that a complex with one ligand bound will not be retained. However, Senear et al. (1986) found no simple relation between j and r_j for specific repressor binding to O_R but did find that the binding of only two or three ligands was sufficient for maximum retention.

To assess the effects of variable retention, separate titrations were conducted with different DNA restriction fragments ranging from 91 to 1749 bp (Figure 6). Clore et al. (1982) derived $k_i = (2^{1/N} - 1)/L_{0.5}$, where k_i and $L_{0.5}$ are the microscopic equilibrium binding constant for nonspecific binding and the ligand concentration for which $\theta = 0.5$ for a DNA of length N in bp. This equation presumes that each liganded DNA complex is retained by the filter with the same efficiency. The curves shown represent the fits to eq 6 in which r_j values were set equal to a constant. That these data are entirely consistent with the presumption of constant retention efficiency is indicated by the fitted k_is, which are the same for all five fragments, both in these and in all similar experiments. By contrast, the data are inconsistent with the relationship $k_i = (2^{1/N} - 1)/(2^{1/N}\zeta - 1)L_{0.5}$, which is correct if the parameter ζ accounts for retention below 100% (Woodbury & von Hippel, 1983).

Further evidence for constant retention of liganded complexes derives from two observations. First, when constant retention is assumed, the fitted k_is from different experiments

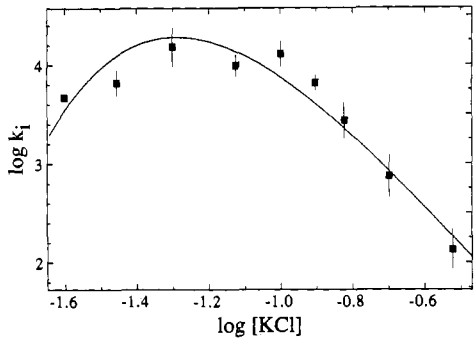

FIGURE 7: log–log plot of [KCl] dependence of nonspecific binding of repressor at 20 °C, pH 7.0, standard assay buffer. Points plotted are microscopic equilibrium constants for the intrinsic binding of repressor to DNA, estimated by analysis of filter binding titration data using eq 6 as described in the text. Error bars represent standard deviations from multiple (2–3) determinations at each condition. Solid lines are the results of analysis using eq 8–10, as described in the text. Parameters are listed in Table III.

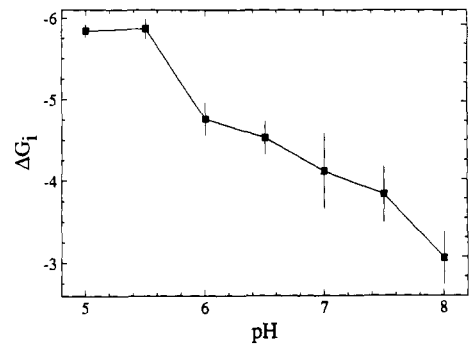

FIGURE 8: Proton-linked effect on nonspecific *c*I repressor–DNA binding at 20 °C, 200 mM KCl, standard conditions. Points plotted are Gibbs free energy changes for the intrinsic binding of repressor to DNA estimated by analysis of filter binding titration data using eq 6 as described in the text. Error bars represent standard deviations from multiple (3–4) determinations at each condition.

are the same (Figure 6, inset) and are independent of the maximum retention. In the particular examples shown, the retention differs by nearly 3-fold. By contrast, analysis of these data using $1 - \xi^j$ to account for the observed retention leads to k_js that vary systematically with maximum observed retention. Second, we find no difference in maximum retention in parallel experiments conducted with the 91 and 1749 bp fragments. The former is large enough to bind only four to five repressor ligands. These results do not rule out the possibility of variable retention dependent on j for $j < 4$. However, in practice, this does not produce a large effect on fitted k_js for filter binding experiments using the 1749 bp fragment. On the basis of these results, filter binding assays using the 1749 bp fragment were analyzed by using constant r_j in eq 6, to determine the [KCl] and pH effects on nonspecific binding. In addition, eq 6 was truncated to the first five terms, as suggested by Clore et al. (1982). We have independently confirmed that the truncated and complete equations are equal to within 0.1%.

[KCl] Dependence of Nonspecific Repressor–DNA Interactions. The effect of [KCl] on the nonspecific binding of the repressor to the 1749 bp pBR322 DNA fragment is shown in Figure 7. The points plotted represent the apparent or averaged microscopic nonspecific binding constant, as defined above. Each data point represents the mean of several measurements at that KCl concentration. Again, Mg^{2+} and Ca^{2+} were included in the buffers in order to match the conditions used for the DNase I footprints (above). The general features of this plot are in common with the O_R binding data in Figure 4. These features include decreased affinity with increased salt concentration, indicative of the effect of ion release, and pronounced curvature at low [KCl]. In this case, the curvature is sufficient to produce a positive slope below about 50 mM KCl. The limiting slope of this plot at high [KCl], which is indicative of the KCl effect alone, is of the same order as the limiting slopes for the KCl effect on the specific binding of repressor to O_R.

pH Dependence of Nonspecific Repressor–DNA Interactions. The pH dependence of nonspecific binding is in Figure 8. Again, the points plotted represent the mean of many measurements. Binding affinity increases with increased proton concentration, indicating that repressor binding is accompanied by net proton absorption. The plateau at low pH indicates saturation in both DNA-bound and DNA-unbound states of the ionizable groups at which proton binding is linked to the protein–DNA interaction. No similar plateau is evident at high pH. However, it proved impossible to conduct experiments above pH 8, due to the low affinity of repressor for DNA. The pH titration (Figure 8) is very similar to that previously observed for repressor binding to O_R (Senear & Ackers, 1990), except that the magnitude of the pH effect in the acid range is smaller.

Discussion

The aim of these studies is to delineate the roles of ion and proton binding in the sequence-specific recognition of DNA by λ *c*I repressor. Specificity is important to λ regulation both at the level of the discrimination of operator DNA and at the level of differential affinity for different operators. This mandates the study both of cooperative, site-specific repressor–O_R interactions and of nonspecific repressor binding.

For nonspecific binding studies, nitrocellulose filter binding has largely been supplanted by more powerful spectral techniques, e.g., circular dichroism (Hurstel et al., 1990), intrinsic fluorescence [cf. Hard et al. (1990), Kleinschmidt et al. (1988), and Takahashi et al. (1989)], fluorescence lifetimes (hard et al., 1989), and fluorescence anisotropy (Takahashi et al., 1990). Attempts to use circular dichroism and fluorescence for these studies were unsuccessful, due to precipitation of the nonspecific protein–DNA complexes, even at low binding density. Studies of *c*I repressor selfpolymerization using fluorescence anisotropy suggest, as an explanation, that *c*I repressor tetramers form at the high concentrations necessary for significant nonspecific binding densities (Ross and Senear, unpublished observations). The bidendate tetramers are presumably efficient DNA cross-linkers.

Filter binding provides a generally useful solution to this problem. Binding to large DNA fragments is assayed at repressor concentrations substantially below the half-saturation point. As has been comprehensively discussed (Woodbury & von Hippel, 1983), it is extremely difficult to obtain all of the parameters necessary to a complete description of nonspecific protein–DNA interactions from filter binding data. The use of large DNA fragments avoids many of the difficulties in interpretation and provides reasonable estimates of the intrinsic affinity of repressor for nonoperator DNA. It also has the unfortunate consequence that it precludes assessment of cooperativity in nonspecific binding.

Two observations argue that the observed titrations are not dominated by semispecific binding to a few, relatively high-affinity sites that might be present. First, no pBR322 sequence has significant similarity to O_R. Second, the data shown in Figure 6 are indicative of strict proportionality between fragment length and binding stoichiometry. The DNA frag-

ments used are blunt-ended, which eliminates the possibility of binding to single-stranded overhangs, as was observed for RNA polymerase (Melancon et al., 1983). Therefore, it is reasonable to interpret the k_is obtained as reflecting averaged intrinsic binding affinity to mixed-sequence DNA.

Salt Dependence of Specific and Nonspecific Binding. Comparison of the KCl effects on binding to the operator sites of O_R and to nonspecific DNA shows apparent differences in the slopes of log–log plots (Figures 4 and 7). These slopes reflect counterion removal from the DNA upon repressor binding. The observed differences suggest a role for ion binding in site-specific recognition. A pronounced effect of millimolar Mg^{2+} and Ca^{2+} is evident in the curvature of the log–log plots. In order to obtain the KCl dependence alone, it is necessary to quantitatively account for this effect.

Record et al. (1977) developed the appropriate theory by considering Mg^{2+} binding to DNA as a competing equilibrium. If anion effects are neglected, this gives

$$\log K_{obsd} = \log K^0 - m\Psi \log [K^+] - m \log ([D]/[D_0]) \quad (8)$$

The first two terms on the right define the effect of K^+ alone, as the limiting straight line at high [KCl]. K_{obsd} and K^0 are observed and reference-state nonspecific equilibrium association constants for repressor, respectively, Ψ is the fraction of counterion (K^+) per phosphate that is thermodynamically associated with DNA (Manning, 1978), and m is the number of counterions (K^+) displaced due to repressor binding (Record et al., 1978). The Mg^{2+} effect is expressed by the last term, in which $[D_0]/[D]$ represents the probability of a nucleotide with its normal complement of K^+, but no associated Mg^{2+}. At low protein binding density, $[D]/[D_0]$ depends on $[Mg^{2+}]$ according to

$$[D]/[D_0] = (1/2)\{1 + (1 + 4K^{Mg}_{obsd}[Mg^{2+}])^{1/2}\} \quad (9)$$

The apparent binding constant for Mg^{2+}, K^{Mg}_{obsd}, is a function of [KCl] according to

$$\log K^{Mg}_{obsd} = \log K^{Mg}_0 - 2\Psi \log [K^+] \quad (10)$$

In applying this formalism to extract the correct slope, $m\Psi$, of the [KCl] dependence at the limit of high [KCl], 2Ψ was fixed equal to its theoretical value of −1.76 (Record et al., 1978). This is justified by close agreement between theoretical and empirically determined values [see Record et al. (1977) and Lohman et al. (1980) and references cited therein]. Also in agreement with Record et al. (1977) and Lohman et al. (1980), we find the fit at low [KCl] to be extremely sensitive to the value $\log K^{Mg}_0$, requiring that this value be fitted to the data. Because the data do not justify separate adjustable parameters, $\log K^{Mg}_0$ and $\log K^{Ca}_0$, we take the further expedient of combining these to a single adjustable parameter, $\log K^{M^{2+}}_0$, describing a concentration-averaged binding constant for the two ions.

This approach is justified by satisfactory agreement between the fitted curves and the data. Equations 8–10 predict that the slope of the KCl effect will become positive at sufficiently low [KCl], an effect which is quite evident in the nonspecific binding data of Figure 7. In molecular terms, this comes about due to stronger competition for binding to DNA between divalent cations and proteins than between monovalent cations and proteins. We obtain $\log K^{M^{2+}}_0 = -0.3 \pm 0.2$ for these data, in agreement with the expectation that it be near zero [see Record et al. (1977) and Lohman et al. (1980) and references cited therein]. The limiting slope at high [KCl], which indicates the number of ions released on binding of the repressor to DNA, is found to be -4.8 ± 0.8. To within the limits of experimental uncertainty, this slope is the same as that of the best straight line through the data above 75 mM KCl.

Table III: M^{2+} and KCl Effects on *c*I Repressor Protein–DNA Binding[a]

parameter	O_R1	O_R2	O_R3	nonspecific
$\log K_0$	11.5 ± 0.2	10.6 ± 0.3	9.1 ± 0.2	4.9 ± 0.3
m	−5.9 ± 0.7	−6.2 ± 0.6	−3.8 ± 0.7	−4.8 ± 0.7
$\log K^M_0$	−1.1 ± 0.2	*c*		−0.3 ± 0.1
σ^b	0.27	*c*		0.19

[a] Parameters from analysis of the log–log plots of salt effects on both operator-specific and nonspecific binding of the *c*I repressor protein, using eq 8–10. Data for operator-specific (Figure 4) and for nonspecific binding (Figure 7) were separately analyzed. Data for operator sites O_R1, O_R2, and O_R3 were simultaneously analyzed. [b] Square root of the variance of the fitted curves. [c] Parameters not separately determined for each site.

The O_R data were analyzed in a similar manner. The three operator site titrations were analyzed simultaneously to a common value, $\log K^{M^{2+}}_0$, but unique $\log K_0$ and m (eq 8) values for each operator. Parameters obtained for nonspecific and for operator binding are compared in Table III.[6] The nonspecific and specific binding data were not fitted to a common value of $\log K^{M^{2+}}_0$ because of their substantially different curvature at the lowest [KCl] concentrations used. This might be due to a different competition with M^{2+}, as reflected in the value of $\log K^{M^{2+}}_0$. It might also reflect an experimental aritifact. The apparent curvature of the nonspecific titration depends heavily on the determination of $\log k_i$ at 25 mM KCl. Steady-state fluorescence anisotropy experiments (Ross and Senear, unpublished observations) suggest the likelihood of significant aggregation of repressor at this low [KCl], and at the relatively high concentrations used in the experiments. This would yield systematically low values of $\log k_i$.

The parameters listed in Table III indicate modest limiting slopes for the KCl dependence.[7] The imprecision of the estimates of m for O_R1 and O_R2 shows any apparent difference to be uncertain. That m values for O_R3 and for nonspecific DNA differ from these as well as from one another is clear. These differences translate directly into contributions to the intrinsic free energy change for binding. It is significant that the ion-dependent contributions neither are constant nor do they scale with the intrinsic binding free energy change. For example, at our standard conditions of pH 7.0 and 200 mM KCl, $\Delta G_3 - \Delta G_1$ is about 2.8 kcal/mol (Table II). Ion effects account for about 1.5 kcal/mol of this difference. By contrast, there appears to be little or no contribution (ca. -0.3 ± 0.6

[6] In analyzing the [KCl] dependence, d log k_d/d log [KCl] was assumed constant (see Materials and Methods). Both theory and empirical studies support this assumption [cf. Aune et al. (1971)]. We have explored whether this assumption affects the limiting slopes (m) at high [KCl] for the repressor–DNA interactions, reported in Table III. We find that while different values of k_d and different relations, $\log k_d = f(\log [KCl])$, do slightly affect both the ΔG_i's at low [KCl] and the M^{2+}-induced curvature of the log–log plots for O_R, there is little effect on m for either operator or nonspecific binding [compare $m = 5.8 \pm 0.9$ for O_R1, d log k_d/d log [KCl] = 0, and $k_d = 20$ nM to $m = -5.9 \pm 0.7$ (Table III), d log k_d/d log [KCl] = −1.5, and $k_d = 3.7$ nM at 200 mM KCl] and essentially no effect on the relationships between the different slopes for the different operators and nonoperator DNA.

[7] This determination of m for O_R1 is similar to that reported by Nelson and Sauer (1985), who obtained -4.8 ± 0.4 from filter binding experiments using $O_R2^{-3^-}$ DNA (created by deletion), and assumed a repressor dimer dissociation constant $k_d = 20$ nM. When analyzed by using this assumption, the data in Figure 4 yield $m = -5.8 \pm 0.9$. Brenowitz et al. (1989) showed that deletion of O_R2 and O_R3 substantially alters the affinity of repressor for O_R1. Together with the observation that m is not constant for different operators, the small discrepancy between our value and that of Nelson and Sauer (1985) appears reasonable.

kcal/mol) to $\Delta G_2 - \Delta G_1$, though it is of similar magnitude to $\Delta G_3 - \Delta G_1$. Only other forces are involved. Therefore, the contributions from ion effects reflect details of the interaction of the repressor with each particular operator sequence and are not related either to the site size (which we take to be constant for the three operators) or to the overall free energy change for the interaction. The contribution from ion effects to the nearly 8 kcal/mol difference in free energy between binding to O_R1 and to nonspecific DNA is also quite small (ca. 1 kcal/mol). This appears inconsistent with the possibility of different binding modes involving, for example, significantly different conformations of the repressor–DNA interface, for nonspecific and operator binding.

Mossing and Record (1985) have also found DNA sequence-dependent ion effects in their observation of up to 2-fold changes in *m* for *lac* repressor binding single base pair operator mutants. The magnitude of the thermodynamic effects, in that instance, suggested to the authors that global changes in interactions, rather than the local loss of favorable interactions or introduction of unfavorable interactions at the mutated base pairs, were involved. Our data point to a similar conclusion. The results of Mossing and Record (1985) implicated ion effects as important in discrimination of mutant operator sequences; our results implicate similar effects as important to the ability of the *c*I repressor to distinguish between the wild-type operators.

In contrast, Nelson and Sauer (1985) interpreted repressor mutants with altered salt dependence for binding to O_R1 in terms of the introduction of additional local repressor–operator interactions. Since binding of the mutants to neither O_R2 nor O_R3 was studied, our results suggest caution in making such interpretations. Similarly, from studies of repressor binding to O_R1 and to a series of operators with changes at the three positions at which O_R1 differs from O_R3, Hochschild et al. (1986) concluded that only two of eight positions of the nonconsensus half-site of O_R1 (positions 3 and 5 of the sequence 5′-TACCTTGG-3′) are primarily responsible for distinguishing O_R1 and O_R3. By implicating an important contribution of ion effects to this affinity difference, our results do not appear to support simple interpretations involving strictly local contacts at these positions.

Salt Dependence of Cooperative Interactions. The free energy changes for cooperative interactions listed in Table II define a significant transition between two ranges of KCl concentration. Above about 0.1 M KCl, the repressor–O_R interactions are highly cooperative, with free energy changes on the order −3.5 to −4.5 kcal/mol, corresponding to 400–2000-fold. Below the transition, the cooperative free energy changes are only about half of this. Note that while ΔG_{12} and ΔG_{23} are approximately equal above 0.1 M KCl, they are unequal below. In addition, ΔG_{12} is slightly KCl dependent below the transition, while ΔG_{23} and ΔG_{123} are not. The reason for the transition is not evident from these data. It was previously observed that the cooperative interactions differ in their linkages to proton absorption (Senear & Ackers, 1990). These observations highlight the uniqueness of these interactions and suggest a linkage between site-specific binding at the different operators and cooperativity.

Cooperativity seems to play a role in maintaining the differential specificity of repressor for the three operators over a wide range of conditions. At high KCl concentration, the intrinsic affinity for O_R2 is relatively low, similar to O_R3. Yet the effective affinity for O_R2 is high, similar to O_R1, due to O_R1–O_R2 cooperativity. Thus, the pattern of cooperative interaction, i.e., O_R1–O_R2 cooperativity, but no O_R1–O_R3 cooperativity (Johnson et al., 1979; Senear & Ackers, 1990), appears to play a greater role in differential affinity for the operators than do intrinsic affinity differences for O_R2 and O_R3. Since the filter binding data provide no information about whether the nonspecific binding of repressor is cooperative, it is useless to speculate whether a linkage between cooperativity and operator site-specific binding might also play a role in specificity at this level. However, such linkage has been observed (Hurstel et al., 1990) and merits consideration in postulating mechanisms for gene regulatory systems.

Table IV: Proton Absorption Linked to *c*I Repressor Binding to DNA[a]

pH	$\Delta\bar{\nu}_H$			
	O_R1	O_R2	O_R3	nonspecific
5.5	1.9 ± 0.3	1.2 ± 0.3	1.2 ± 0.4	0.8 ± 0.1
6.5	0.4 ± 0.3	1.0 ± 0.2	0.5 ± 0.2	0.5 ± 0.3
7.5	0.8 ± 0.2	0.8 ± 0.2	0.8 ± 0.3	0.8 ± 0.4
8.5	1.2 ± 0.3	0.7 ± 0.2	1.5 ± 0.2	nd[b]

[a] Net proton absorption ($\Delta\bar{\nu}_H$) linked to binding of *c*I repressor protein to O_R, and to nonspecific DNA. $\Delta\bar{\nu}_H$, calculated from $\Delta\bar{\nu}_H = d \ln k / d \ln a_{H^+} = (1/2.303RT)[\Delta(\Delta G)/\Delta pH]$, with approximately one standard deviation (estimated by propagation of errors), is shown. The calculations for binding to O_R are based on data of Senear and Ackers (1990) and of Senear and Bolen (1991). The former were corrected to reflect a repressor dimer concentration scale based on a repressor dimer dissociation constant of 3.7 nM (see Materials and Methods), by considering the effect of the change in concentration scale on the midpoints of the individual-site titration curves. Binding to O_R was studied only at integral pH units. Therefore, for direct comparison between specific and nonspecific repressor binding, $\Delta\bar{\nu}_H$ in both cases was calculated by differences between integral pH units, and is reported for the middle of the range. [b] Not determined.

pH Effects on Specific and Nonspecific Binding. Extension of pH-dependent studies of the repressor–O_R interactions to pH 9 (Senear & Bolen, 1991) and studies of the pH dependence of nonspecific binding confirm the role of proton binding (Senear & Ackers, 1990) in sequence-specific recognition. A plateau, or region of pH independence, is observed in the nonspecific binding data at pH 5 defining the affinity of the fully protonated repressor. It is presumed that this behavior also characterizes binding to O_R, although studies at pH 5.5 have not been conducted to confirm this. The slope of the curve in Figure 8 is related to the net proton absorption when the repressor binds nonspecifically to DNA, according to $\Delta\bar{\nu}_H = d \ln k / d \ln a_{H^+}$ (Wyman, 1964). For the number and range of data in Figure 8, this slope is adequately approximated by $(1/2.303RT)[\Delta(\Delta G)/\Delta pH]$, where Δ is the difference between values at two conditions. The results of this calculation are compared to that for repressor binding to O_R in Table IV.

$\Delta\bar{\nu}_H$ is positive over the entire pH range, for both operator and nonoperator DNA, indicating that the pK_a's of ionizable groups increase (become more basic) when repressor binds to DNA. The pattern of $\Delta\bar{\nu}_H$ versus pH, i.e., net proton adsorption that is greater at extremes of pH than near neutral pH, is the same for nonspecific repressor binding as for operator binding. If the pH titrations were the same for the three operators, and for nonspecific DNA, then the pH effect might arise from the titration of the *free* repressor, through a series of states of increasing DNA binding activity, due to increasing positive charge. In this model, the binding free energy change at a given pH would reflect the equilibrium distribution of those states. However, significant differences in $\Delta\bar{\nu}_H$ for the three operator sites at pH 5.5 and smaller differences at 6.5 which were observed previously (Senear & Akers, 1990) are inconsistent with this model. These were interpreted as arising from DNA sequence-dependent pK_a shifts of ionizable repressor groups in the acid range upon binding to DNA.

The nonspecific binding data reported here differ in $\Delta\bar{\nu}_H$ from any of the operators in this same pH range. This confirms the significance of the earlier observations and supports their interpretation. It seems probable that the same ionizable repressor groups make sequence-dependent interactions with both operator and nonspecific DNA. This supports the results of the KCl titrations, which indicate that there are not distinctly different modes of binding to operator and to nonoperator DNA. Differential pH effects in the acid range contribute as much as 0.8–0.9 kcal/mol to the differential affinity of the repressor for the three operators (Senear & Ackers, 1990). However, the contribution to the difference in affinity between nonspecific DNA and O_R3, the lowest affinity operator, is somewhat less, and it is clear that this is not the major contributor to discrimination of operator from nonoperator DNA.

The additional data at pH 9 (Senear & Bolen, 1991) indicate differences between the three operators at high pH also. This is again inconsistent with a molecular interpretation involving *only* the titration of the free repressor. Instead, it implicates pK_a shifts of basic repressor groups which are sensitive to the sequence of the DNA binding site. A reasonable speculation is that the basic groups on the amino-terminal arm of the repressor, which have been shown to be important to site-specific recognition (Pabo et al., 1982; Eliason et al., 1985; Hochschild et al., 1986) and are believed to make sequence-specific contacts, are involved. If so, one might expect a smaller pH effect on nonspecific binding than an operator binding in this range. Low affinity precluded measurement of k_i for nonspecific binding above pH 8. The lack of evidence for a plateau below pH 9 is also noteworthy. This raises the possibility that the pH effect in this range might also in part reflect the titration of free repressor to an unprotonated state which does not bind DNA.

Implications for Sequence Recognition. Structural and mutational studies present a partial picture of the λ *c*I repressor–operator interactions that are responsible for sequence-specific recognition. The repressor/O_L1 cocrystallographic structure (Jordan & Pabo, 1988) highlights specific H-bond contacts with the conserved base pairs at positions 2, 4, and 6 in the major groove of each operator half-site as being crucial to the discrimination of operator sequences. Of course, these interactions cannot account for the differential specificity for the operators. Exhaustive mutagenesis studies (Benson et al., 1988) have also implicated the base pairs at positions 5, 7, and 8 as important to recognition, and base pairs 3 and 5 are implicated in the ability of repressor to distinguish O_R1 from O_R3 (Hochschild et al., 1986). The repressor N-terminal arm has been suggested as being responsible for recognition of bp 8 (Pabo et al., 1982; Jordan & Pabo, 1988), though the details of the interaction are unclear. Interactions with the backbone phosphates observed for bp 5 and 7 (Johnson et al., 1979; Jordan & Pabo, 1988) provide no simple structural interpretation of the base pair preference. Still, the base pair specific contacts that are observed, along with the absence of any major distortion of the DNA helix, have led to the conclusion that direct, local contacts with the edges of the base pairs in the major groove are the principal sources of specificity (Harrison & Aggarwal, 1990).

The observations detailed here support the view that additional indirect effects of DNA sequence are also important components of recogntion by λ repressor. These indirect effects are reflected in both the pH and KCl titrations of operator and of nonspecific DNA. With respect to the pH titrations, the simplest explanation for the similar patterns of $\Delta\bar{\nu}_H$ versus pH for the different operators, and for nonoperator DNA, is that the same ionizable groups are involved. In that case, the differences in $\Delta\bar{\nu}_H$ that are observed are due to pK_a shifts which differ in magnitude for the various repressor–DNA complexes. As discussed by Senear and Ackers (1990), such differences must be due to different conformations of the three repressor–operator complexes and of the repressor–nonspecific DNA complexes. That proton linkages should be similar for operator and nonoperator DNA is consistent with the observation of only subtle perturbations of the DNA conformation in the repressor/O_L1 cocrystallographic structure. Energetically, the contributions of proton binding to site specificity are similar both at the level of operator discrimination and at the level of distinguishing between different operators.

With respect to KCl titrations, it is significant that ion removal does not dominate the difference between operator and nonoperator repressor binding as is frequently the case [cf. Kleinschmidt et al. (1988) and Record and Mossing (1987)]. In contrast to that situation, the *c*I repressor clearly does not exhibit distinctly differently specific and nonspecific binding modes. Like the pH effects, the differential KCl effects that are observed are most simply explained as reflecting different deformations of the repressor, or different conformations of the DNA so that a different number of ions (and presumably water molecules) are removed from the interface upon binding. These experiments were conducted at pH 7, a region devoid of sequence-dependent proton binding. This minimizes the possibility that the differential KCl effects are simply measuring a different repressor charge due to different fractional occupancy of proton binding sites.

Proton absorption and ion release both appear to contribute significantly to site-specific binding to or recognition of O_R1. At O_R2, only ion removal is significant, and at O_R3, only proton absorption is significant. There is no obvious correlation between either the pH or the KCl effects and either the overall binding free energy change or the similarity of the DNA sequence to the operator consensus. Therefore, it does not appear probable that the effects arise from different local contacts. Rather, they must reflect more global changes in the repressor–DNA complex conformations which affect the overall complementarity between protein and DNA. These results highlight both the variability of thermodynamic effects for protein–DNA interactions, even involving similar DNA sites, and the need for additional structural information, e.g., structures of complexes other than repressor/O_L1, if the structural basis for recognition is to be fully understood.

ACKNOWLEDGMENTS

We thank J. B. A. Ross for conducting the steady-state fluorescence anisotropy studies of the repressor monomer–dimer equilibrium. We also gratefully acknowledge M. Thomas Record, Jr., for beneficial discussions and members of our lab, particularly Alan Kanehl and Yao Te Huang, for technical contributions.

Registry No. KCl, 7447-40-7; H, 12408-02-5.

REFERENCES

Ackers, G. K., Johnson, A. D., & Shea, M. A. (1982) *Proc. Natl. Acad. Sci. U.S.A. 79*, 1129–1133.

Ackers, G. K., Shea, M. A., & Smith, F. R. (1983) *J. Mol. Biol. 170*, 223–242.

Aune, K. C., Goldsmith, L. C., & Timasheff, S. N. (1971) *Biochemistry 10*, 1617–1622.

Benson, N., Sugiono, P., & Youderian, P. (1988) *Genetics 118*, 21–29.

Box, G. E. P. (1960) *Ann. N.Y. Acad. Sci. 86*, 792.

Brenowitz, M., & Senear, D. F. (1989) in *Current Protocols in Molecular Biology* (Ausubel, F. M., Brent, R., Kingston, R. E., Moore, D. D., Seidman, J. G., Smith, J. A., & Struhl, K., Eds.) Vol. 2, Suppl. 7, Unit 12.4, Greene Publishing Associates and Wiley-Interscience Associates, New York.

Brenowitz, M., Senear, D. F., Shea, M. A., & Ackers, G. K. (1986) *Methods Enzymol. 130*, 132–181.

Brenowitz, M., Senear, D. F., & Ackers, G. K. (1989) *Nucleic Acids Res. 17*, 3747–3755.

Casali, E., Petra, P. H., & Ross, J. B. A. (1990) *Biochemistry 29*, 9334–9343.

Clore, G. M., Gronenborn, A. M., & Davies, R. W. (1982) *J. Mol. Biol. 155*, 447–466.

Eliason, J. L., Weiss, M. A., & Ptashne, M. (1985) *Proc. Natl. Acad. Sci. U.S.A. 82*, 2339–2343.

Hard, T., Sayre, M. H., Geiduschek, E. P., & Kearns, D. R. (1989) *Biochemistry 28*, 2813–2819.

Hard, T., Dahlman, K., Carlstedt, D. J., Gustafsson, J. A., & Rigler, R. (1990) *Biochemistry 29*, 5358–5364.

Harrison, S. C., & Aggarwal, A. K. (1990) *Annu. Rev. Biochem. 59*, 933–969.

Hildebrand, F. B. (1956) *Introduction to Numerical Analysis*, McGraw-Hill, New York.

Hochschild, A., Douhan, J. I., & Ptashne, M. (1986) *Cell 47*, 807–816.

Hurstel, S., Granger, S. M., & Schnarr, M. (1990) *Biochemistry 29*, 1961–1970.

Johnson, A. D. (1980) Ph.D. Dissertation, Harvard University, Cambridge, MA.

Johnson, A. D., Meyer, B. J., & Ptashne, M. (1979) *Proc. Natl. Acad. Sci. U.S.A. 76*, 5061–5065.

Johnson, A. D., Poteete, A. R., Lauer, G., Sauer, R. T., Ackers, G. K., & Ptashne, M. (1981) *Nature 294*, 217–223.

Johnson, M. L., & Frasier, S. G. (1985) *Methods Enzymol. 117*, 301–342.

Jordan, S. R., & Pabo, C. O. (1988) *Science 242*, 893–899.

Kleinschmidt, C., Tovar, K., Hillen, W., & Porschke, D. (1988) *Biochemistry 27*, 1094–1104.

Kunitz, M. (1950) *J. Gen. Physiol. 33*, 349.

Lohman, T. M., deHaseth, P. L., & Record, M. T., Jr. (1980) *Biochemistry 19*, 3522–3530.

Maniatis, T., Fritsch, E. F., & Sambrook, J. (1982) *Molecular Cloning—A Laboratory Manual*, Cold Spring Harbor Laboratory, Cold Spring Harbor, NY.

Manning, G. S. (1978) *Q. Rev. Biophys. 11*, 179–246.

Melancon, P., Burgess, R. R., & Record, M. T., Jr. (1983) *Biochemistry 22*, 5169.

Meyer, B. J., Maurer, R., & Ptashne, M. (1980) *J. Mol. Biol. 139*, 163–194.

Mossing, M. C., & Record, M. T., Jr. (1985) *J. Mol. Biol. 186*, 295–305.

Nelson, H. C. M., & Sauer, R. T. (1985) *Cell 42*, 549–558.

Pabo, C. O., Krovatin, W., Jeffrey, A., & Sauer, R. T. (1982) *Nature 298*, 441–443.

Record, M. T., Jr., & Mossing, M. C. (1987) in *RNA Polymerase and Regulation of Transcription. Proceedings of the Sixteenth Steenbock Symposium* (Reznikoff, W. S., Burgess, R. R., Dahlberg, J. E., Gross, C. A., Record, M. T., Jr., & Wickens, M. P., Eds.) pp 61–83, Elsevier, New York.

Record, M. T., Jr., deHaseth, P. L., & Lohman, T. M. (1977) *Biochemistry 16*, 4791–4796.

Record, M. T., Jr., Anderson, C. F., & Lohman, T. M. (1978) *Q. Rev. Biophys.* 411, 103–178.

Record, M. T., Jr., Anderson, C. F., Mills, P., Mossing, M., & Roe, J.-H. (1985) *Adv. Biophys. 20*, 109–135.

Sauer, R. T. (1979) Ph.D. Dissertation, Harvard University, Cambridge, MA.

Senear, D. F., & Ackers, G. K. (1990) *Biochemistry 29*, 6568–6577.

Senear, D. F., & Bolen, D. W. (1991) *Methods Enzymol.* in press.

Senear, D. F., Brenowitz, M., Shea, M. A., & Ackers, G. K. (1986) *Biochemistry 25*, 7344–7354.

Shea, M. A., & Ackers, G. K. (1985) *J. Mol. Biol. 181*, 211–230.

Steitz, T. A. (1990) *Q. Rev. Biophys. 23*, 205–280.

Strahs, D., & Brenowitz, M. (1990) *Biophys. J. 57*, 70a.

Takahashi, M., Blazy, B., Baudras, A., & Hillen, W. (1989) *J. Mol. Biol. 207*, 783–796.

Takahashi, M., Sakumi, K., & Sekiguchi, M. (1990) *Biochemistry 29*, 3431–3436.

Woodbury, C. P. J., & von Hippel, P. H. (1983) *Biochemistry 22*, 4730–4737.

Wyman, J. (1964) *Adv. Protein Chem. 19*, 223–286.